39th AIAA Fluid Dynamics Conference
22 - 25 June 2009, San Antonio, Texas

AIAA 2009-4162

Reynolds Stress Closure Including Nonlocal and Nonequilibrium Effects in Turbulent Flows

Peter E. Hamlington and Werner J.A. Dahm
Laboratory for Turbulence & Combustion (LTC)
Department of Aerospace Engineering, The University of Michigan
Ann Arbor, MI, 48109-2140, USA

A new Reynolds stress anisotropy closure that includes nonlocal and nonequilibrium effects in turbulent flows has been obtained from a recently proposed nonlocal anisotropy formulation. This formulation is based on a new nonlocal derivation of the rapid pressure-strain correlation, which rigorously accounts for nonlocal effects on the anisotropy due to spatial variations in the mean velocity gradient tensor. The present nonlocal and nonequilibrium anisotropy model is obtained as a quasi-linear solution to the anisotropy transport equation, and directly replaces the classical local equilibrium Boussinesq closure in standard two-equation turbulence models. This allows straightforward implementation of the present approach in existing computational frameworks for solving the Reynolds averaged Navier-Stokes equations. Here we present the first assessment of the model in inhomogeneous flows – where nonlocal effects are expected to be important – by comparing with results from direct numerical simulations of turbulent channel flow.

I. Introduction

Due to the often prohibitive computational resources required for large eddy simulations (LES) and direct numerical simulations (DNS) of even relatively basic turbulent flows, the vast majority of simulations for practical problems will continue to be done within the Reynolds-averaged Navier-Stokes (RANS) framework. The single-point RANS equations are obtained from the continuity and momentum equations as

$$\frac{\partial \rho}{\partial t} + \frac{\partial \left(\rho \overline{u}_i\right)}{\partial x_i} = 0\,, \tag{1}$$

$$\rho \frac{D\overline{u}_i}{Dt} = -\frac{\partial \overline{p}}{\partial x_i} + \frac{\partial}{\partial x_j}\left[2\mu \overline{S}_{ij} - \frac{2}{3}\mu \overline{S}_{nn}\delta_{ij} - \rho \overline{u_i' u_j'}\right]\,, \tag{2}$$

where D/Dt is the mean flow material derivative and $\overline{S}_{ij}$ is the mean strain rate tensor, defined as

$$\overline{S}_{ij} \equiv \frac{1}{2}\left(\frac{\partial \overline{u}_i}{\partial x_j} + \frac{\partial \overline{u}_j}{\partial x_i}\right)\,. \tag{3}$$

In order to solve (1)-(3), a closure model for the Reynolds stress tensor $\overline{u_i' u_j'}$ appearing in (2) is required. This can be written in terms of its isotropic ($\frac{2}{3}k\delta_{ij}$) and anisotropic parts as

$$\overline{u_i' u_j'} = \frac{2}{3}k\delta_{ij} - \left(\overline{u_i' u_j'}\right)_{aniso}\,, \tag{4}$$

where $k \equiv \frac{1}{2}\overline{u_i' u_i'}$ is the turbulence kinetic energy. The anisotropic part is equivalently written in terms of the Reynolds stress anisotropy tensor a_{ij}, defined as

$$a_{ij} \equiv -\frac{(\overline{u_i' u_j'})_{aniso}}{k} = \frac{\overline{u_i' u_j'}}{k} - \frac{2}{3}\delta_{ij}\,, \tag{5}$$

and closing the system in (1)-(3) requires a suitable model for the anisotropy in (5).

The evolution of the anisotropy in turbulent flows fundamentally involves nonlocal and nonequilibrium effects, both of which must be accurately predicted in order to provide high-fidelity solutions of the RANS equations in (1)-(3). Here *nonlocality* refers to a pressure-based effect arising from the pressure-strain correlation in the exact transport equation for the anisotropy.[1,2] The nonlocal nature of the anisotropy evolution can also be seen from the double Biot-Savart representation for the Reynolds stresses, namely

$$\overline{u_i' u_j'}(\mathbf{x},t) = \frac{1}{4\pi}\int_{-\infty}^{\infty}\frac{1}{4\pi}\int_{-\infty}^{\infty}\epsilon_{ikl}\epsilon_{jmn}\,\overline{\omega_k'(\check{\mathbf{x}},t)\omega_m'(\hat{\mathbf{x}},t)}\frac{(x_l-\check{x}_l)}{|\mathbf{x}-\check{\mathbf{x}}|^3}\frac{(x_n-\hat{x}_n)}{|\mathbf{x}-\hat{\mathbf{x}}|^3}\,d\check{\mathbf{x}}\,d\hat{\mathbf{x}}\,, \tag{6}$$

where the stresses depend on the two-point vorticity fluctuation correlation at all points in the flow. Due to the strong spatial variations of mean flow quantities in the wall-normal direction, nonlocal effects are particularly significant in wall bounded flows, although other inhomogeneous flows (e.g. free shear flows) also involve a certain degree of nonlocality.

Nonequilibrium effects on the anisotropy evolution have been discussed elsewhere,[3] and are fundamentally tied to the importance of Lagrangian history effects on the local anisotropy. That is, the anisotropy at any location and time depends on the prior history of the anisotropy along mean-flow pathlines. Nonequilibrium effects are perhaps most obvious in unsteadily strained homogeneous turbulence, where the anisotropy does not respond instantly to changes in the applied strain (for example in impulsively[4] and periodically[5] sheared turbulence), although nonequilibrium effects are also significant in strongly inhomogeneous flows where flow properties can vary dramatically along mean pathlines (for example across shock waves in compressible flows).

Despite the importance of nonlocal and nonequilibrium effects in even relatively basic problems however, nearly all prior models for the anisotropy neglect nonlocal effects, including second-order Reynolds stress transport models. Moreover, nonequilibrium effects are neglected in the most widely used linear and nonlinear eddy viscosity models (the assumptions used to obtain these and other models are summarized in a number of comprehensive reviews[6,7]). In particular, the overwhelmingly popular standard $k-\epsilon$ and $k-\omega$ two-equation models are based on the classical equilibrium Boussinesq closure, which assumes the anisotropy to be directly proportional to the local instantaneous mean strain rate tensor, namely

$$a_{ij} = -2\frac{\nu_T}{k}\overline{S}_{ij}\,, \tag{7}$$

where ν_T is the eddy viscosity. Despite the widespread popularity of models based on (7), the direct dependence on $\overline{S}_{ij}$ in (7) explicitly neglects nonlocal and nonequilibrium effects on the anisotropy.

In the following we depart from prior approaches and develop a new anisotropy closure that includes both nonlocal and nonequilibrium effects in turbulent flows, but does so within a relatively simple approach that is readily implemented in existing two-equation frameworks for solving (1)-(3). The present closure seeks to include the principal nonequilibrium dynamics of a_{ij} contained in full Reynolds stress transport models, while additionally accounting for nonlocal effects due to spatial variations in the mean strain rate tensor. This is accomplished by solving a quasi-linearized form of a recently proposed[1] nonlocal anisotropy transport equation that is based on a new nonlocal representation for the rapid pressure-strain correlation. The resulting model for the anisotropy replaces the *local instantaneous* mean strain rate $\overline{S}_{ij}$ appearing in the Boussinesq hypothesis with a *nonlocal, nonequilibrium effective* strain rate $\widetilde{S}_{ij}$. The purely nonequilibrium form of this tensor was originally proposed in Ref. [3], and in the following the effective strain is extended to include nonlocal effects on the anisotropy evolution. The present closure is shown in the following to provide good agreement with results from DNS of fully-developed turbulent channel flow, where strong spatial variations in the near-wall region lead to substantial nonlocal effects on the anisotropy.

II. Formulation of the Nonlocal Anisotropy Transport Equation

The present anisotropy closure for nonlocal and nonequilibrium effects is obtained from a recently proposed[1] nonlocal transport equation for the anisotropy. This transport equation is based on a new nonlocal formulation for the rapid pressure-strain correlation in turbulent flows, and allows more accurate predictions of the anisotropy in the presence of strong spatial variations in the mean velocity gradient field.

II.A. Exact Anisotropy Transport Equation

From the definition of the Reynolds stress anisotropy in (5), the exact anisotropy transport equation can be obtained from

$$\frac{Da_{ij}}{Dt} = \frac{1}{k}\left(\frac{D\overline{u_i'u_j'}}{Dt} - \frac{\overline{u_i'u_j'}}{k}\frac{Dk}{Dt}\right). \tag{8}$$

On the right-hand side, the transport equation for the Reynolds stresses $\overline{u_i'u_j'}$ can be written[6] as

$$\frac{D\overline{u_i'u_j'}}{Dt} = P_{ij} + \Pi_{ij} - \epsilon_{ij} + D_{ij}\,. \tag{9}$$

In (9), P_{ij} is the production tensor

$$P_{ij} \equiv -\overline{u_i'u_l'}\frac{\partial \overline{u}_j}{\partial x_l} - \overline{u_j'u_l'}\frac{\partial \overline{u}_i}{\partial x_l}\,, \tag{10}$$

Π_{ij} is the pressure-strain rate correlation tensor given by

$$\Pi_{ij}(\mathbf{x}) \equiv \frac{2}{\rho}\,\overline{p'(\mathbf{x})S_{ij}'(\mathbf{x})}\,, \tag{11}$$

with the fluctuating strain rate tensor S_{ij}' defined as

$$S_{ij}' \equiv \frac{1}{2}\left(\frac{\partial u_i'}{\partial x_j} + \frac{\partial u_j'}{\partial x_i}\right), \tag{12}$$

ϵ_{ij} is the dissipation rate tensor given by

$$\epsilon_{ij} \equiv 2\nu\overline{\frac{\partial u_i'}{\partial x_l}\frac{\partial u_j'}{\partial x_l}}\,, \tag{13}$$

and D_{ij} accounts for viscous, turbulent, and pressure transport and is defined as

$$D_{ij} \equiv -\frac{\partial}{\partial x_l}\left(\overline{u_i'u_j'u_l'} + \overline{\frac{p'}{\rho}u_j'}\delta_{li} + \overline{\frac{p'}{\rho}u_i'}\delta_{jl} - \nu\frac{\partial \overline{u_i'u_j'}}{\partial x_l}\right). \tag{14}$$

The corresponding transport equation for the turbulence kinetic energy k is obtained from the trace of (9) as

$$\frac{Dk}{Dt} = P - \epsilon + D\,, \tag{15}$$

where $P \equiv P_{nn}/2$, $D \equiv D_{nn}/2$, $\epsilon \equiv \epsilon_{nn}/2$, and $\Pi_{nn} \equiv 0$ in incompressible turbulence. Substituting (9) and (15) into (8), and employing the definition of the anisotropy in (5), gives the exact anisotropy transport equation

$$\frac{Da_{ij}}{Dt} = -\left(\frac{P}{\epsilon} - 1\right)\frac{\epsilon}{k}a_{ij} + \frac{1}{k}\left[P_{ij} - \frac{2}{3}P\delta_{ij}\right] + \frac{1}{k}\Pi_{ij} - \frac{1}{k}\left[\epsilon_{ij} - \frac{2}{3}\epsilon\delta_{ij}\right] + \frac{1}{k}\left[D_{ij} - \left(a_{ij} + \frac{2}{3}\delta_{ij}\right)D\right]. \tag{16}$$

The production term in (16) can be fully expanded in terms of a_{ij}, $\overline{S}_{ij}$, and the antisymmetric part of the mean velocity gradient tensor $\overline{W}_{ij}$, defined as

$$\overline{W}_{ij} \equiv \frac{1}{2}\left(\frac{\partial \overline{u}_i}{\partial x_j} - \frac{\partial \overline{u}_j}{\partial x_i}\right), \tag{17}$$

to obtain the exact form

$$\left[P_{ij} - \frac{2}{3}P\delta_{ij}\right] = -\frac{4}{3}k\overline{S}_{ij} - k(a_{il}\overline{S}_{lj} + \overline{S}_{il}a_{lj} - \frac{2}{3}a_{nl}\overline{S}_{nl}\delta_{ij}) + k(a_{il}\overline{W}_{lj} - \overline{W}_{il}a_{lj})\,, \tag{18}$$

where the kinetic energy production P is given by

$$P = -k\,a_{ij}\,\overline{S}_{ij}\,. \tag{19}$$

With (18), the exact transport equation for a_{ij} is then

$$\frac{Da_{ij}}{Dt} = -\left(\frac{P}{\epsilon}-1\right)\frac{\epsilon}{k}a_{ij} - \frac{4}{3}\overline{S}_{ij} - \left(a_{il}\overline{S}_{lj} + \overline{S}_{il}a_{lj} - \frac{2}{3}a_{nl}\overline{S}_{nl}\delta_{ij}\right) \tag{20}$$
$$+ \left(a_{il}\overline{W}_{lj} - \overline{W}_{il}a_{lj}\right) + \frac{1}{k}\Pi_{ij} - \frac{1}{k}\left[\epsilon_{ij} - \frac{2}{3}\epsilon\delta_{ij}\right] + \frac{1}{k}\left[D_{ij} - \left(a_{ij} + \frac{2}{3}\delta_{ij}\right)D\right] .$$

In (20), k is given by (15), P is given by (19), and the remaining unclosed terms are Π_{ij}, ϵ_{ij}, and D_{ij}. The dissipation is here given by its high-Reynolds number isotropic form, namely

$$\epsilon_{ij} = \frac{2}{3}\epsilon\delta_{ij} , \tag{21}$$

and a number of standard models for D_{ij} have been summarized in Ref. [6]. Thus, the only remaining unclosed term in (20) is the pressure-strain correlation Π_{ij}.

II.B. Pressure-Strain Correlation Π_{ij}

Nearly all models for the pressure-strain correlation Π_{ij}, defined in (11), are typically related to the exact integral for the pressure fluctuation p', which is obtained from the Poisson equation[8]

$$\frac{1}{\rho}\nabla^2 p' = -2\frac{\partial\overline{u}_k}{\partial x_l}\frac{\partial u'_l}{\partial x_k} - \frac{\partial^2}{\partial x_k \partial x_l}\left(u'_k u'_l - \overline{u'_k u'_l}\right) . \tag{22}$$

This equation permits the Green's function solution[9]

$$\frac{1}{\rho}p'(\mathbf{x}) = \frac{1}{4\pi}\int_{\mathbf{R}}\left[2\frac{\partial\overline{u}_k}{\partial\hat{x}_l}\frac{\partial u'_l}{\partial\hat{x}_k} + \frac{\partial^2}{\partial\hat{x}_k\partial\hat{x}_l}\left(u'_k u'_l - \overline{u'_k u'_l}\right)\right]_{\hat{\mathbf{x}}}\frac{d\hat{\mathbf{x}}}{|\mathbf{x}-\hat{\mathbf{x}}|} , \tag{23}$$

and from (11) and (23) Π_{ij} is then given by

$$\Pi_{ij}(\mathbf{x}) = \frac{1}{2\pi}\int_{\mathbf{R}}\overline{\left[2\frac{\partial\overline{u}_k}{\partial\hat{x}_l}\frac{\partial u'_l}{\partial\hat{x}_k} + \frac{\partial^2}{\partial\hat{x}_k\partial\hat{x}_l}\left(u'_k u'_l - \overline{u'_k u'_l}\right)\right]_{\hat{\mathbf{x}}} S'_{ij}(\mathbf{x})}\frac{d\hat{\mathbf{x}}}{|\mathbf{x}-\hat{\mathbf{x}}|} , \tag{24}$$

where the integration spans the entire flow domain $\mathbf{R}$. Beginning with Chou,[9] it has been common to write p' in terms of slow, rapid, and wall parts as

$$p' = p'^{(s)} + p'^{(r)} + p'^{(w)} , \tag{25}$$

defined by their respective Poisson equations from (22) as

$$\frac{1}{\rho}\nabla^2 p'^{(s)} = -\frac{\partial^2}{\partial x_k\partial x_l}\left(u'_k u'_l - \overline{u'_k u'_l}\right) , \tag{26}$$

$$\frac{1}{\rho}\nabla^2 p'^{(r)} = -2\frac{\partial\overline{u}_k}{\partial x_l}\frac{\partial u'_l}{\partial x_k} , \tag{27}$$

$$\frac{1}{\rho}\nabla^2 p'^{(w)} = 0 . \tag{28}$$

The effect of $p'^{(w)}$ is significant only in the extreme near-wall region of wall-bounded flows[8,10] and will not be considered further in the following. The remaining $p'^{(s)}$ and $p'^{(r)}$ parts produce corresponding slow and rapid contributions, here denoted by $\Pi^{(s)}_{ij}$ and $\Pi^{(r)}_{ij}$, respectively, to the pressure-strain correlation Π_{ij} in (11), with Green's function solutions of (26) and (27) giving these as

$$\Pi^{(s)}_{ij}(\mathbf{x}) = \frac{1}{2\pi}\int_{\mathbf{R}}\overline{\frac{\partial^2\left(u'_k u'_l\right)_{\hat{\mathbf{x}}}}{\partial\hat{x}_k\partial\hat{x}_l}S'_{ij}(\mathbf{x})}\frac{d^3\hat{\mathbf{x}}}{|\mathbf{x}-\hat{\mathbf{x}}|} , \tag{29}$$

$$\Pi^{(r)}_{ij}(\mathbf{x}) = \frac{1}{\pi}\int_{\mathbf{R}}\frac{\partial\overline{u}_k(\hat{\mathbf{x}})}{\partial\hat{x}_l}\overline{\frac{\partial u'_l(\hat{\mathbf{x}})}{\partial\hat{x}_k}S'_{ij}(\mathbf{x})}\frac{d^3\hat{\mathbf{x}}}{|\mathbf{x}-\hat{\mathbf{x}}|} . \tag{30}$$

With the relation $\Pi_{ij} = \Pi^{(s)}_{ij} + \Pi^{(r)}_{ij}$, the integrals in (29) and (30) provide an exact representation for Π_{ij} in (20), although developing fundamentally-based yet practically implementable forms for $\Pi^{(s)}_{ij}$ and $\Pi^{(r)}_{ij}$ from (29) and (30) remains one of the primary challenges in turbulence research.

II.C. Nonlocal Form of the Rapid Pressure-Strain Correlation $\Pi_{ij}^{(r)}$

While purely local representations for $\Pi_{ij}^{(s)}$ and $\Pi_{ij}^{(r)}$ have been used to formulate a number of relatively successful second-order Reynolds stress transport (e.g. Launder, Reece, and Rodi[11] and Speziale, Sarkar, and Gatski[12]) and algebraic stress (e.g. Gatski and Speziale,[13] Girimaji,[14] and Wallin and Johansson[15]) models, these approaches fundamentally assume that the mean velocity gradient in (30) is homogeneous. By contrast, the approach developed herein accounts for effects due to spatial variations in the mean velocity gradient on the rapid correlation $\Pi_{ij}^{(r)}$ through Taylor expansion of $\overline{u}_k(\hat{\mathbf{x}})/\partial x_l$ in (30) about the point $\mathbf{x}$. This gives

$$\frac{\partial \overline{u}_k(\mathbf{r}+\mathbf{x})}{\partial r_l} = A_{kl}(\mathbf{x}) + r_m \frac{\partial A_{kl}(\mathbf{x})}{\partial x_m} + \frac{1}{2} r_m r_p \frac{\partial^2 A_{kl}(\mathbf{x})}{\partial x_m \partial x_p} + \cdots + \frac{1}{n!} \left(r_m r_p \ldots\right) \frac{\partial^n A_{kl}}{\partial x_m \partial x_p \ldots} + \cdots , \tag{31}$$

where $\mathbf{r} \equiv \hat{\mathbf{x}} - \mathbf{x}$, n is the order of the expansion, and for convenience we have defined $A_{kl}(\mathbf{x}) \equiv \partial \overline{u}_k(\mathbf{x})/\partial x_l$. It can be shown that substitution of (31) into (30) then yields

$$\Pi_{ij}^{(r)}(\mathbf{x}) = \sum_{n=0}^{\infty} \left[\frac{\partial^n A_{kl}(\mathbf{x})}{\partial x_m \partial x_p \ldots}\right] \left[{}_{(mp\ldots)}M_{iljk}^{(n)}(\mathbf{x}) + {}_{(mp\ldots)}M_{jlik}^{(n)}(\mathbf{x})\right] , \tag{32}$$

with

$${}_{(mp\ldots)}M_{iljk}^{(n)}(\mathbf{x}) \equiv -\frac{1}{2\pi n!} \int_{-\infty}^{\infty} \left[\frac{r_m r_p \ldots}{r^n}\right] r^{n-1} \frac{\partial^2 R_{il}(\mathbf{x},\mathbf{r})}{\partial r_j r_k} d\mathbf{r} , \tag{33}$$

where $R_{il}(\mathbf{r})$ denotes the two-point velocity fluctuation correlation

$$R_{il}(\mathbf{r}) \equiv \overline{u_i'(\mathbf{x}) u_l'(\mathbf{r}+\mathbf{x})} . \tag{34}$$

For the nth-order term in (32) there are n derivatives of A_{kl} as well as n total indices $(mp\ldots)$ in ${}_{(mp\ldots)}M_{iljk}^{(n)}$. Implementation of (32) in (20) thus requires a solution for the ${}_{(mp\ldots)}M_{iljk}^{(n)}$ integrals in (33).

The principal hypothesis in the present approach is that the nonlocality in the rapid pressure-strain correlation is substantially due to spatial variations in A_{kl}, and in order to address these effects the velocity fluctuation correlation $R_{il}(\mathbf{r})$ can be given by its homogeneous isotropic form, namely

$$R_{il}(r) = \frac{2}{3} k \left[f(r)\delta_{il} + \frac{r}{2}\frac{df}{dr}\left(\delta_{il} - \frac{r_i r_l}{r^2}\right)\right] , \tag{35}$$

with

$$f(r) \equiv \frac{3}{2} \frac{\overline{u'(\mathbf{x}+\mathbf{r}) u'(\mathbf{x})}}{k} , \tag{36}$$

where k is the turbulence kinetic energy. It can be shown[1] using (35) in (33) that

$$\begin{aligned} {}_{(mp\ldots)}M_{iljk}^{(n)} = -\frac{k}{6\pi n!} \Bigg[&\int_0^{\infty} r^n \frac{df}{dr} dr \int_{\Omega} a_{ijkl} \frac{r_m r_p \ldots}{r^n} \, d\Omega + \int_0^{\infty} r^{n+1} \frac{d^2 f}{dr^2} dr \int_{\Omega} b_{ijkl} \frac{r_m r_p \ldots}{r^n} \, d\Omega \\ &+ \int_0^{\infty} r^{n+2} \frac{d^3 f}{dr^3} dr \int_{\Omega} c_{ijkl} \frac{r_m r_p \ldots}{r^n} \, d\Omega \Bigg] , \end{aligned} \tag{37}$$

where $d\Omega = \sin\theta \, d\theta \, d\phi$, and the coefficients a_{ijkl}, b_{ijkl}, and c_{ijkl} are defined as

$$a_{ijkl} \equiv 3\delta_{jk}\delta_{il} - \delta_{ij}\delta_{kl} - \delta_{jl}\delta_{ki} - 3\alpha_{jk}\delta_{il} + \delta_{ij}\alpha_{lk} + \delta_{jl}\alpha_{ik} + \delta_{ik}\alpha_{lj} + \delta_{kl}\alpha_{ij} + \delta_{kj}\alpha_{il} - 3\beta_{iljk} , \tag{38a}$$

$$b_{ijkl} \equiv \delta_{il}\delta_{jk} + 3\alpha_{jk}\delta_{il} - \delta_{ij}\alpha_{lk} - \delta_{lj}\alpha_{ik} - \delta_{ik}\alpha_{lj} - \delta_{kl}\alpha_{ij} - \delta_{kj}\alpha_{il} + 3\beta_{iljk} , \tag{38b}$$

$$c_{ijkl} \equiv \delta_{il}\alpha_{jk} - \beta_{iljk} , \tag{38c}$$

with

$$\alpha_{ij} \equiv \frac{r_i r_j}{r^2} , \quad \beta_{ijkl} \equiv \frac{r_i r_j r_k r_l}{r^4} . \tag{39}$$

Solution of the integrals over r in (37) requires a representation for the longitudinal correlation function $f(r)$ defined in (36). Using the standard high-Reynolds number exponential approximation for $f(r)$, namely

$$f(r/\Lambda) = e^{-r/\Lambda}\,, \tag{40}$$

where

$$\Lambda \equiv C_\lambda \frac{k^{3/2}}{\epsilon} \tag{41}$$

is the integral length scale, as shown in Ref. [1] solution of (37) yields the final result

$$\Pi_{ij}^{(r)} = k \sum_{n=1}^{\infty} C_2^{(n)} \Lambda^{2n-2} \left(\nabla^2\right)^{n-1} \overline{S}_{ij}\,, \tag{42}$$

where the coefficients $C_2^{(n)}$ are given by

$$C_2^{(n)} = \frac{16n^2 - 16n + 36}{3(2n+3)(4n^2-1)}\,. \tag{43}$$

The formulation in (42) and (43) accounts for nonlocal effects on the rapid correlation $\Pi_{ij}^{(r)}$ due to spatial variations in the mean velocity gradient tensor. The principal approximation used in the derivation is the high-Reynolds number representation for $f(r)$ in (40), although it has been shown[1] through comparisons with experimental and computational data that this representation is relatively accurate in a variety of free shear and wall bounded flows.

II.D. The Nonlocal Anisotropy Transport Equation

Combining $\Pi_{ij}^{(r)}$ in (42) with the standard local representation for $\Pi_{ij}^{(s)}$, namely[16]

$$\frac{1}{k}\Pi_{ij}^{(s)} = -C_1 \frac{\epsilon}{k} a_{ij}\,, \tag{44}$$

and the higher-order anisotropic terms found in most prior pressure-strain models (e.g. Refs. [11,12])

$$\frac{1}{k}\Pi_{ij}^{(aniso)} = C_3 \left(a_{il}\overline{S}_{lj} + \overline{S}_{il}a_{lj} - \frac{2}{3}a_{nl}\overline{S}_{nl}\delta_{ij} \right) + C_4 \left(a_{il}\overline{W}_{lj} - \overline{W}_{il}a_{lj} \right)\,, \tag{45}$$

we obtain a nonlocal model for Π_{ij} as

$$\begin{aligned} \frac{1}{k}\Pi_{ij} = -C_1 \frac{\epsilon}{k} a_{ij} + \sum_{n=1}^{\infty} \left[C_2^{(n)} \Lambda^{2n-2} \left(\nabla^2\right)^{n-1} \overline{S}_{ij} \right] \\ -C_3 \left(a_{il}\overline{S}_{lj} + \overline{S}_{il}a_{lj} - \frac{2}{3}a_{nl}\overline{S}_{nl}\delta_{ij} \right) + C_4 \left(a_{il}\overline{W}_{lj} - \overline{W}_{il}a_{lj} \right)\,, \end{aligned} \tag{46}$$

where the $C_2^{(n)}$ coefficients are given by (43). The anisotropic terms in (45) are required to account for the fact that (42) is obtained using the isotropic formulation for $R_{il}(\mathbf{r})$ in (35). The model in (46) accounts for nonlocal effects due to spatial variations in the mean strain rate tensor, and in homogeneous flows, for which local models of Π_{ij} are relatively successful, all Laplacians of $\overline{S}_{ij}$ in (46) are zero and the model recovers prior purely local forms.

With the isotropic formulation for ϵ_{ij} in (21), the nonlocal pressure-strain correlation in (46) can be incorporated in the exact a_{ij} transport equation in (20) to give

$$\begin{aligned} \frac{Da_{ij}}{Dt} = & - \alpha_1 \frac{\epsilon}{k} a_{ij} + \alpha_2 \overline{S}_{ij} + \sum_{n=2}^{\infty} \left[C_2^{(n)} \Lambda^{2n-2} \left(\nabla^2\right)^{n-1} \overline{S}_{ij} \right] \\ & + \alpha_3 \left(a_{il}\overline{S}_{lj} + \overline{S}_{il}a_{lj} - \frac{2}{3}a_{nl}\overline{S}_{nl}\delta_{ij} \right) + \alpha_4 \left(a_{il}\overline{W}_{lj} - \overline{W}_{il}a_{lj} \right) + \frac{1}{k}\left[D_{ij} - \left(a_{ij} + \frac{2}{3}\delta_{ij} \right) D \right]\,, \end{aligned} \tag{47}$$

where once again the $C_2^{(n)}$ coefficients are defined in (43) and the α_i are given by

$$\alpha_1 = \frac{P}{\epsilon} - 1 + C_1\,, \quad \alpha_2 = C_2^{(1)} - \frac{4}{3}\,, \quad \alpha_3 = C_3 - 1\,, \quad \alpha_4 = C_4 - 1\,. \tag{48}$$

We do not specify new values of C_1, C_3, and C_4 here, and standard values of these coefficients can be found elsewhere.[11,12] The equation in (47) is thus a new nonlocal anisotropy transport equation that accounts for nonlocal effects due to spatial variations in the mean strain rate tensor.

III. Present Anisotropy Model for Nonlocal and Nonequilibrium Effects

A number of different approaches can be taken for solving (47). First, (47) can be solved as a complete set of six coupled partial differential equations to obtain a new nonlocal Reynolds stress transport model that improves upon existing approaches (e.g. Refs. [11,12]) in strongly inhomogeneous flows. Second, the Da_{ij}/Dt term on the left-hand side of (47) can be neglected to obtain a nonlocal algebraic stress model similar to those developed, for example, by Gatski and Speziale,[13] Girimaji,[14] and Wallin and Johansson.[15] However, in the following Da_{ij}/Dt will be retained in (47) to obtain a new computationally simple representation for the anisotropy that accounts for both nonlocal and nonequilibrium effects in turbulent flows.

III.A. Quasi-Linear Nonlocal Anisotropy Transport Equation

As discussed previously,[3,17] quasi-linearization of the anisotropy dynamics is sufficient to retain the most important dynamics governing the evolution of the anisotropy in the majority of common problems. This quasi-linearization is physically motivated by the substantial linearity of the vorticity dynamics in turbulent flows,[18] where the Reynolds stress anisotropy is rigorously connected to the vorticity through the relation in (6).

Retaining only the first three terms on the right-hand side of (47) gives a nonlocal quasi-linear equation for the anisotropy evolution as

$$\frac{Da_{ij}}{Dt} = -\frac{1}{\Lambda_m} a_{ij} + \alpha_2 \overline{S}_{ij} + \sum_{n=2}^{\infty} \left[C_2^{(n)} \Lambda^{2n-2} \left(\nabla^2\right)^{n-1} \overline{S}_{ij} \right]\,, \tag{49}$$

where the $C_2^{(n)}$ coefficients are given in (43), α_2 is given in (48), and we have denoted the resulting turbulence memory time scale Λ_m as

$$\Lambda_m \equiv C_\Lambda \frac{k}{\epsilon} \quad \text{with} \quad C_\Lambda \equiv \frac{1}{\alpha_1}\,. \tag{50}$$

Despite the dependence of α_1 on P/ϵ, as noted in (48), a constant value for C_Λ has been determined previously as[3] $C_\Lambda = 0.26$.

While the nonlocal quasi-linear equation in (49) lacks many of the higher-order nonlinear interactions in (47), it still contains the principal dynamics governing the evolution of the anisotropy in most common turbulence problems. The equation in (49) contains a "slow" ($-a_{ij}/\Lambda_m$), a "fast" ($\alpha_2 \overline{S}_{ij}$), and a nonlocal (via the Laplacians of $\overline{S}_{ij}$) contribution to the anisotropy evolution. The "fast" term accounts for the direct response of the turbulence to changes in the mean strain, while the "slow" term accounts for the decreasing effect over time of the prior straining history on the local anisotropy. The nonlocal term in (49) accounts for the effects of spatial variations in the mean strain on the anisotropy evolution, and has not been addressed by prior closure approaches.

III.B. The Nonlocal Effective Strain Rate Tensor

Here we will integrate (49) directly to obtain a relatively simple anisotropy model that can be readily implemented in conventional two-equation frameworks for closing the RANS equations in (1)-(3). Defining the nonlocal tensor T_{ij} as

$$T_{ij} \equiv \overline{S}_{ij} + \sum_{n=2}^{\infty} \left[\frac{C_2^{(n)}}{\alpha_2} \Lambda^{2n-2} \left(\nabla^2\right)^{n-1} \overline{S}_{ij} \right]\,, \tag{51}$$

the quasi-linear equation in (49) is solved exactly as

$$a_{ij}(t) = \int_{t_0}^{t} \alpha_2 T_{ij}(\tau) h(t-\tau) D\tau + a_{ij}(t_0) \exp\left[-\int_{t_0}^{t} \frac{1}{\Lambda_m(t')} Dt' \right], \tag{52}$$

where t_0 is the initial time and $h(t-\tau)$ is the impulse response function that represents the effective "memory" of the turbulence, namely

$$h(t-\tau) \equiv \exp\left[-\int_{\tau}^{t} \left[\Lambda_m(t')\right]^{-1} Dt' \right]. \tag{53}$$

The histories of both T_{ij} and the time scale Λ_m along mean-flow pathlines are accounted for in (52) and (53). Expanding the inverse of the relaxation time scale $\Lambda_m(t')$ around the current time t and integrating, (53) can be written as

$$h(t-\tau) = \exp\left[-\frac{(t-\tau)}{\Lambda_m(t)} + \frac{1}{2}(t-\tau)^2 \frac{D\left(1/\Lambda_m\right)}{Dt} + \ldots \right]. \tag{54}$$

Here it is assumed that the derivative terms in (54) are negligible relative to the leading term, thus ignoring the explicit time history of Λ_m in the a_{ij} dynamics. However, the history of Λ_m in (50) is still accounted for indirectly through the dynamical equations for k and ϵ found in most standard two-equation model frameworks.

Setting $t_0 \to -\infty$ and assuming $a_{ij}(-\infty) \equiv 0$, the solution for a_{ij} from (52) becomes a convolution integral of the form

$$a_{ij}(t) = \int_{-\infty}^{t} \alpha_2 T_{ij}(\tau) e^{-(t-\tau)/\Lambda_m(t)} D\tau \,. \tag{55}$$

By noting[13] that C_μ in standard linear eddy viscosity models is related to the α_i in (48) as $C_\mu \equiv -\alpha_2/2\alpha_1$, the convolution in (55) can be equivalently written, with (50), as

$$a_{ij}(t) = -2C_\mu \frac{k}{\epsilon} \frac{1}{\Lambda_m(t)} \int_{-\infty}^{t} T_{ij}(\tau) e^{-(t-\tau)/\Lambda_m(t)} D\tau \,. \tag{56}$$

Since $\Lambda_m(t)$ is a constant with respect to the integration variable τ, the effective strain tensor $\widetilde{S}_{ij}$ can be defined as

$$\widetilde{S}_{ij}(t) = \int_{-\infty}^{t} T_{ij}(\tau) \frac{e^{-(t-\tau)/\Lambda_m(t)}}{\Lambda_m(t)} D\tau \,, \tag{57}$$

in terms of which the nonlocal, nonequilibrium anisotropy closure can be written in a form analogous to the traditional equilibrium Boussinesq hypothesis in (7) as

$$a_{ij}(t) = -2\frac{\nu_T}{k} \widetilde{S}_{ij}(t) \,, \tag{58}$$

where the eddy viscosity ν_T is defined in the context of a $k-\epsilon$ model as $\nu_T = C_\mu k^2/\epsilon$. From (51) and (57), the nonlocal effective strain rate $\widetilde{S}_{ij}$ is written in terms of $\overline{S}_{ij}$ as

$$\widetilde{S}_{ij} = \int_{-\infty}^{t} \overline{S}_{ij}(\tau) \frac{e^{-(t-\tau)/\Lambda_m(t)}}{\Lambda_m(t)} D\tau + \sum_{n=2}^{\infty} \frac{C_2^{(n)}}{\alpha_2} \int_{-\infty}^{t} \left[\Lambda^{2n-2} \left(\nabla^2\right)^{n-1} \overline{S}_{ij} \right]_\tau \frac{e^{-(t-\tau)/\Lambda_m}}{\Lambda_m} D\tau \,. \tag{59}$$

It is possible[3] to write the convolution integrals in (57) and (59) in purely time local form through Taylor expansion of T_{ij} about the current time t, which gives

$$\begin{aligned} \widetilde{S}_{ij}(t) = \overline{S}_{ij}(t) &+ \sum_{m=1}^{\infty} (-\Lambda_m)^m \left. \frac{D^m \overline{S}_{ij}}{Dt^m} \right|_t + \sum_{n=2}^{\infty} \left[\frac{C_2^{(n)}}{\alpha_2} \Lambda^{2n-2} \left(\nabla^2\right)^{n-1} \overline{S}_{ij} \right]_t \\ &+ \sum_{n=2}^{\infty} \sum_{m=1}^{\infty} \frac{C_2^{(n)}}{\alpha_2} (-\Lambda_m)^m \frac{D^m}{Dt^m} \left[\Lambda^{2n-2} \left(\nabla^2\right)^{n-1} \overline{S}_{ij} \right]_t . \end{aligned} \tag{60}$$

The first term on the right-hand side of (60) is the equilibrium response of the anisotropy to the mean strain $\overline{S}_{ij}$ found in the local equilibrium Boussinesq closure in (7). The second term on the right in (60) accounts for

nonequilibrium effects in the flow, while the third term accounts for nonlocal effects due to spatial variations in the mean velocity gradient. The last term in (60) is a mixed term that addresses both nonequilibrium and nonlocal effects, and is only expected to be significant in flows that exhibit both strong nonequilibrium and inhomogeneity. The form for $\widetilde{S}_{ij}$ in (60) is appropriate for implementation in existing computational frameworks for solving (1)-(3), where typically only local and instantaneous flow variables are available.

The closure in (58) with (59) or (60) thus accounts for nonequilibrium effects via the history-dependent convolution integrals (or material derivatives D/Dt), as well as spatially nonlocal effects via the Laplacians of $\overline{S}_{ij}$. In homogeneous flows, all Laplacians of $\overline{S}_{ij}$ are zero and the second term on the right-hand side of (59), and the third and fourth terms on the right-hand side of (60), can be neglected. The resulting formulation for $\widetilde{S}_{ij}$ is then identical to the previously derived[3] purely nonequilibrium model for the anisotropy.

III.C. Practical Implementation of Nonlocal, Nonequilibrium Closure

As a practical matter, implementation of the nonlocal, nonequilibrium closure in (58) with (60) in existing computational frameworks requires calculation of numerous Laplacians and material derivatives of $\overline{S}_{ij}$. However, these higher-order derivatives may lead to stability issues associated with solving (1)-(3) in engineering simulations, and will certainly increase the required computational resources. Consequently, in nearly all applications of the present closure, it will be necessary to truncate the series expansions in (60) at finite n and m for which computational issues are not expected to be prohibitive.

While the exact truncation order of the series in (60) is ultimately determined by the specific user, application, and available computing resources, truncation of (60) imposes restrictions on the limits of the r integrals in (37) and the τ integrals in (57) or (59). The present approach accounts for nonlocal effects in the rapid pressure-strain correlation through Taylor expansion of $A_{kl}(\hat{\mathbf{x}})$ about the point $\mathbf{x}$, which gives the series in (32) with the integral coefficients in (37). Similarly, the time-local nonequilibrium effects in (60) (given by the D/Dt terms) are obtained through Taylor expansion of $T_{ij}(\tau)$ in (57) about the current location and time $(\mathbf{x}, t)$. However, truncating the series (60) is equivalent to truncating the expansions for $A_{kl}(\hat{\mathbf{x}})$ and $T_{ij}(\tau)$, and this can result in errors for the representations of $A_{kl}(\hat{\mathbf{x}})$ and $T_{ij}(\tau)$ outside a certain region centered on $\mathbf{x}$ and t. In order to avoid these errors, we here replace the infinite limits on the integrals in (37) and (57) with finite bounds related to the order of the expansions for $A_{kl}(\hat{\mathbf{x}})$ and $T_{ij}(\tau)$. For truncations of (32) at order N, we integrate r in (37) from 0 to the length scale R, and for truncations of the expansion for T_{ij} at order M we replace $-\infty$ in the lower integration bound of (57) with the parameter Γ. Both R and Γ are related to the orders N and M of the expansions, as well as to the degree of local variation in A_{kl} and T_{ij}. In general, only for $N \to \infty$ and $M \to \infty$ can we set $R \to \infty$ and $\Gamma \to -\infty$.

It can be shown that integration of the r integrals in (37) from 0 to R using the exponential $f(r)$ in (40) gives

$$\Pi_{ij}^{(r)} = k \sum_{n=1}^{N} C_2^{(n)} \Lambda^{2n-2} \left(\nabla^2\right)^{n-1} \overline{S}_{ij} \,, \tag{61}$$

where N denotes the order of the truncation and the coefficients $C_2^{(n)}$ are now written as

$$C_2^{(n)} = \frac{32n}{3(2n+3)(2n-1)} \left[\gamma_1^{(2n-2)}(R/\Lambda)\right] + \frac{4(2n-9)}{3(2n+3)} \left[\gamma_2^{(2n-2)}(R/\Lambda)\right] - \frac{8n(2n-5)}{3(2n+3)(2n+1)} \left[\gamma_3^{(2n-2)}(R/\Lambda)\right] , \tag{62}$$

with

$$\gamma_j^{(n)}(x) \equiv 1 - e^{-x} \sum_{i=1}^{n+j} \frac{x^{n+j-i}}{(n+j-i)!} \,. \tag{63}$$

As shown in Figure 1, for any n the $\gamma_j^{(n)}$ coefficients are bounded by 0 and 1, and behave as damping functions. In the limit $R/\Lambda \to \infty$ in (62), (63) gives simply $\gamma_j^{(n)} = 1$. As the order n increases, the $\gamma_j^{(n)}$ coefficients in Fig. 1 decrease for any particular value of R/Λ. As a result, for finite R/Λ the higher-order n terms make a relatively smaller contribution to the final result.

Integration of (57) from Γ to t using the time-local series expansion[3] for T_{ij} in the integrand then gives

$$\widetilde{S}_{ij}(t) = \sum_{m=0}^{M} (-\Lambda_m)^m \frac{D^m T_{ij}}{Dt^m} \left[\gamma_1^{(m)} \left(\frac{t-\Gamma}{\Lambda_m}\right)\right] , \tag{64}$$

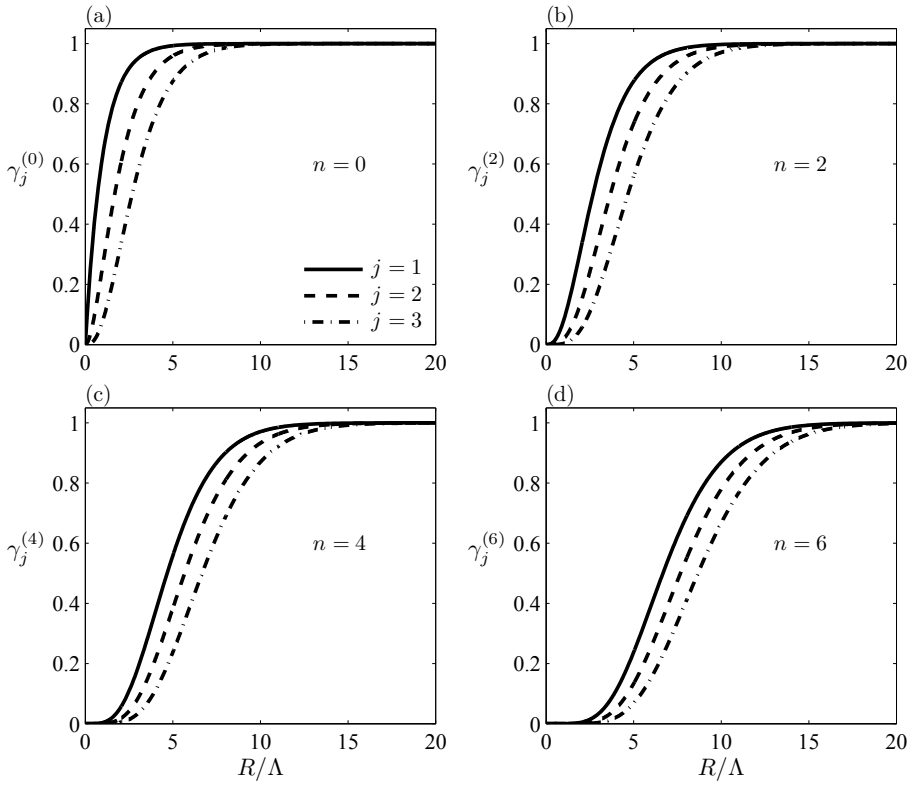

Figure 1. Parameter $\gamma_j^{(n)}$ from (63) as a function of R/Λ for $n = 0$ (a), $n = 2$ (b), $n = 4$ (c), and $n = 6$ (d).

where the damping function $\gamma_1^{(m)}$ is defined in (63). For $\Gamma \to -\infty$ we obtain $\gamma_1^{(m)} \to 1$, and the result in (60) is recovered. By analogy with the coefficients $C_2^{(n)}$ in (61), we can define

$$B^{(m)} \equiv \gamma_1^{(m)} \left(\frac{t - \Gamma}{\Lambda_m} \right) , \tag{65}$$

which from (64) gives

$$\widetilde{S}_{ij}(t) = B^{(0)} \left[T_{ij} + \sum_{m=1}^{M} \frac{B^{(m)}}{B^{(0)}} \left(-\Lambda_m \right)^m \frac{D^m T_{ij}}{Dt^m} \right] . \tag{66}$$

Using (61)-(63) and (66), the nonlocal, nonequilibrium effective strain rate $\widetilde{S}_{ij}$ in (60) can thus be written as

$$\begin{aligned} \widetilde{S}_{ij}(t) = \overline{S}_{ij}(t) + \sum_{m=1}^{M} \frac{B^{(m)}}{B^{(0)}} \left(-\Lambda_m \right)^m \left. \frac{D^m \overline{S}_{ij}}{Dt^m} \right|_t + \sum_{n=2}^{N} \left[\frac{C_2^{(n)}}{\alpha_2} \Lambda^{2n-2} \left(\nabla^2 \right)^{n-1} \overline{S}_{ij} \right]_t \\ + \sum_{n=2}^{N} \sum_{m=1}^{M} \frac{C_2^{(n)}}{\alpha_2} \frac{B^{(m)}}{B^{(0)}} (-\Lambda_m)^m \frac{D^m}{Dt^m} \left[\Lambda^{2n-2} \left(\nabla^2 \right)^{n-1} \overline{S}_{ij} \right]_t , \end{aligned} \tag{67}$$

where N and M are the highest orders of the series expansions, the $C_2^{(n)}$ are defined in (62), and the $B^{(m)}$ are defined in (65). With (67) the anisotropy closure is still given by (58), where $C_2^{(1)}$ and $B^{(0)}$ have been absorbed into the definition of the eddy viscosity ν_T.

III.D. Representation for Radius of Convergence R

Closure of the anisotropy using (58) with (67) requires formulations for R appearing in the $C_2^{(n)}$ coefficients given by (62), and for Γ appearing in the $B^{(m)}$ coefficients given by (65). While the parameter Γ is important

in nonequilibrium turbulent flows, here we focus simply on the representation for R, which is most relevant for the fully-developed turbulent channel flow tests of the present closure presented in the next section.

As noted in Section III.C, R is fundamentally determined by competition between two opposing effects, one physical and the other practical. From a physical standpoint, R should be as large as possible in order to obtain good agreement between the result in (61) with (62) and the full integral solution for $\Pi_{ij}^{(r)}$ in (30), which is strictly defined as an integral over $(-\infty, \infty)$. This would suggest that good agreement requires $R \to \infty$, or at the very least $R \gg \Lambda$. At the same time however, the largest allowable value of R is practically limited by the size of the region in which truncations of (31) are good approximations to the exact $A_{kl}(\mathbf{x}+\mathbf{r})$. Fundamentally, the accuracy of the approximation at any point is determined by both the order N and the smoothness of A_{kl} near the point of interest. In general, the allowable R increases as N increases, or the local inhomogeneity in A_{kl} decreases. Conversely, for small N or rapidly varying A_{kl} the allowable R will generally become relatively small. Only in the limit $N \to \infty$ does the allowable radius R go to ∞.

Thus, we can make the following exact statement: *R is strictly defined as the radius of the* largest *spherical region centered on $\boldsymbol{x}$ in which the Nth-order truncation of (31) is in good agreement with the exact value of $A_{kl}(\boldsymbol{x}+\boldsymbol{r})$ within the region.* To obtain good agreement with the integral in (30), R should ideally be greater than Λ, although this condition may be impractical for the relatively small N permitted by the available computational resources and issues of stability. As a result, a good approximation to the full integral for $\Pi_{ij}^{(r)}$ in (30) may be obtained for values of R near Λ. In the following we will let $R \propto \Lambda$, and consequently the ratio R/Λ appearing in the $\gamma_j^{(n)}$ damping coefficients in (63) is constant everywhere in the flow. It will be seen from comparisons with DNS of fully-developed turbulent channel flow that for truncation at $N = 2$ in (67), the value

$$\frac{R}{\Lambda} = 0.85\,, \tag{68}$$

is sufficient to give good agreement with DNS results down to $y^+ \approx 16$ in the near-wall region.

IV. Tests in Fully-Developed Turbulent Channel Flow

In order to assess the accuracy of the new anisotropy closure given by (58) with (60) or (67), here we consider fully-developed turbulent channel flow, for which nonequilibrium effects can be neglected (an assessment of the nonequilibrium aspects of the present closure are presented in Refs. [3,17]). The equilibrium Boussinesq hypothesis provides relatively accurate predictions of the anisotropy in this flow near the channel centerline, but substantially over-predicts the anisotropy magnitude in the near-wall region where the mean shear varies dramatically. This failure is due in large part to the neglect of nonlocal effects in the pressure-strain formulation.

In the following we will use results from various channel flow DNS studies in order to assess the accuracy of the nonlocal rapid pressure strain correlation and the resulting nonlocal, nonequilibrium anisotropy closure. We first show how a nonlocal *equilibrium* closure can be obtained from (58) with (60) or (67). This closure is then applied to the log-layer region for which an analytical study can be performed, and then finally the nonlocal closure is evaluated using DNS of various fully-developed turbulent channel flow test cases.

It should be noted that while the present closure is expected to provide improved predictions for the anisotropy in any flow with a spatially varying mean velocity gradient field, the turbulent channel flow is a particularly attractive validation case due to the availability of a number of high-quality DNS databases. From a practical standpoint, calculation of the higher-order Laplacians of $\overline{S}_{ij}$ in (60) requires high-resolution validation data, and such data is simply not currently available for other canonical inhomogeneous flows, such as the turbulent jet and mixing layer.

IV.A. Present Closure in Equilibrium Turbulent Flows

The anisotropy closure in (58) expresses a_{ij} in terms of the effective strain $\widetilde{S}_{ij}$, which is defined as a convolution integral over the nonlocal tensor T_{ij} in (57). The effective strain accounts for both nonlocal and nonequilibrium effects on the anisotropy in turbulent flows. For turbulent flows near equilibrium however, the turbulence memory time scale Λ_m is, by definition, much less than the time scale over which T_{ij} varies. For the purposes of the present analysis, we can denote this latter time scale by Λ_T. In such equilibrium flows the representation for $\widetilde{S}_{ij}$ in (57) becomes greatly simplified, and in particular nonequilibrium history effects on the anisotropy evolution can be neglected in the closure representation.

The nonlocal equilibrium closure can be formally derived by taking the limit of $\widetilde{S}_{ij}$ in (57) as $(\Lambda_m/\Lambda_T) \to 0$. Making the change of variables $x = -(t-\tau)/(\Lambda_m/\Lambda_T)$, (57) can be rewritten as

$$\widetilde{S}_{ij}(t) = \int_{-\infty}^{0} T_{ij}\left(t + \frac{\Lambda_m}{\Lambda_T}x\right)\frac{e^{x/\Lambda_T}}{\Lambda_T}dx\,. \tag{69}$$

In the limit $\Lambda_m/\Lambda_T \to 0$, (69) then yields the equilibrium relation

$$\lim_{\Lambda_m/\Lambda_T \to 0} \widetilde{S}_{ij}(t) = T_{ij}(t)\,, \tag{70}$$

and consequently there is no longer any history-dependence in $\widetilde{S}_{ij}$.

With (70) and the definition of T_{ij} in (51), the nonlocal equilibrium anisotropy closure is obtained from (58) as

$$a_{ij} = -2\frac{\nu_T}{k}\left[\overline{S}_{ij} + \sum_{n=2}^{N}\frac{C_2^{(n)}}{\alpha_2}\Lambda^{2n-2}\left(\nabla^2\right)^{n-1}\overline{S}_{ij}\right], \tag{71}$$

where the $C_2^{(n)}$ are given by (43) for $N \to \infty$ and (62) for finite N, with $\alpha_2 = C_2^{(1)} - 4/3$. The first term in the square brackets is the local equilibrium response of the anisotropy, which corresponds to the equilibrium Boussinesq hypothesis in (7). By contrast to the Boussinesq hypothesis however, the series of Laplacians in (71) additionally accounts for nonlocal effects due to inhomogeneities in the mean strain rate tensor. It will be seen herein from tests in fully developed turbulent channel flow that these additional terms give dramatically improved agreement with DNS results when compared to results from the local equilibrium Boussinesq hypothesis.

IV.B. Log-Layer Analysis

Before detailed quantitative comparisons are made with DNS validation data, we can first carry out an analytical assessment of the nonlocal terms in (71) through consideration of the anisotropy in the channel flow log-layer. Within this layer the velocity is given by

$$u^+ = \frac{1}{\kappa}\ln y^+ + B\,, \tag{72}$$

where $\kappa = 0.41$, $B = 5.2$, and u^+ and y^+ are defined as

$$u^+ = \frac{\overline{u}}{u_\tau}, \quad y^+ = \frac{yu_\tau}{\nu}\,. \tag{73}$$

The profile in (72) generally shows good agreement with DNS and experimental results well into the near-wall region,[8] often down to $y^+ \approx 30$. Within the log-layer, the mean shear $\overline{S}_{12}$ is given from (73) as

$$\overline{S}_{12} = \frac{1}{2}\frac{\partial\overline{u}}{\partial y} = \frac{1}{2}\frac{u_\tau^2}{\nu}\frac{\partial u^+}{\partial y^+} = \frac{1}{2}\frac{u_\tau^2}{\nu}\frac{1}{\kappa y^+}\,. \tag{74}$$

and the shear anisotropy a_{12} from (71) is thus given by

$$a_{12} = -2\frac{\nu_T}{k}\overline{S}_{12}\left[1 - \frac{17}{21}\left(\frac{\Lambda^+}{y^+}\right)^2 - \frac{44}{7}\left(\frac{\Lambda^+}{y^+}\right)^4 - \frac{11400}{77}\left(\frac{\Lambda^+}{y^+}\right)^6 + \cdots\right], \tag{75}$$

where $\Lambda^+ \equiv \Lambda u_\tau/\nu$ and the $C_2^{(n)}$ coefficients from (43) have been used to obtain the result. By contrast, the Boussinesq hypothesis in (7) gives the anisotropy in the log-layer as

$$a_{12} = -2\frac{\nu_T}{k}\overline{S}_{12}\,. \tag{76}$$

Comparison of (75) with (76) shows that the magnitude of a_{12} is reduced in the log-layer by the nonlocal correction terms. As will be seen in the following DNS comparisons, the Boussinesq hypothesis drastically over-predicts the anisotropy magnitude in the near-wall region, and the reduction in the magnitude of a_{12} from (75) may thus be sufficient to give better agreement with DNS.

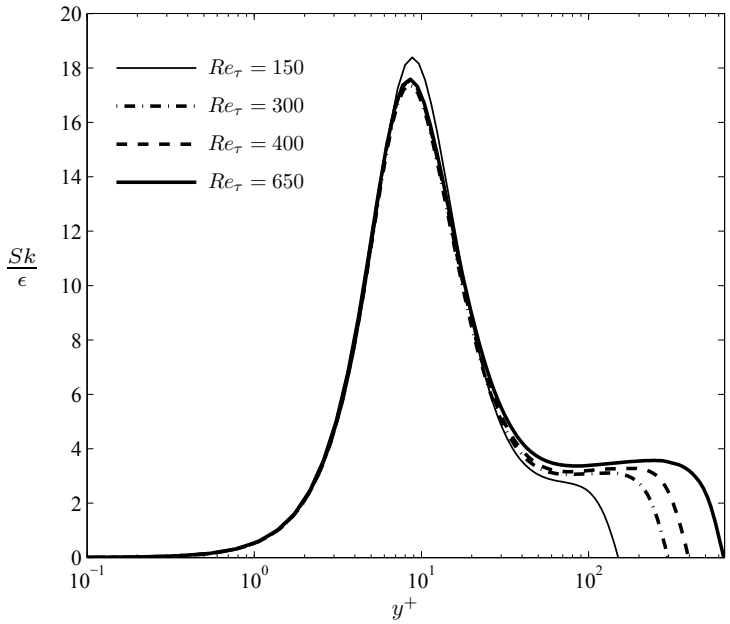

Figure 2. Nondimensional shear parameter Sk/ϵ as a function of y^+ in fully developed turbulent channel flow from DNS by Iwamoto *et al.*[19]

IV.C. Comparisons with DNS

In the following, eight different Reynolds numbers from three different fully-developed turbulent channel flow DNS databases are examined. The Reynolds number cases considered herein are (*i*) $Re_\tau = 150$, 300, 400, 650 from Iwamoto *et al.*,[19] (*ii*) $Re_\tau = 180$ and 395 from Moser *et al.*,[20] and (*iii*) $Re_\tau = 550$ and 950 from Hoyas and Jimenez.[21] Perhaps the main advantage of using these DNS databases for testing the present closure is that all flow variables, including k and ϵ, are provided exactly. The specific closure relation for the anisotropy can thus be tested without concerns about the representations for the additional turbulence variables.

As discussed in Section III.C, as higher-order terms are retained in (71), an increasing number of Laplacians of $\overline{S}_{ij}$ must be calculated. However, the resolution of the DNS becomes an issue for large N, and in the following we will consider the $N = 2$ truncation of (71), which gives

$$a_{ij} = -2\frac{\nu_T}{k}\left[\overline{S}_{ij} + \frac{C_2^{(2)}}{\left(C_2^{(1)} - 4/3\right)}\Lambda^2\nabla^2\overline{S}_{ij}\right], \tag{77}$$

where

$$C_2^{(1)} = \frac{32}{15}\gamma_1^{(0)}(R/\Lambda) - \frac{28}{15}\gamma_2^{(0)}(R/\Lambda) + \frac{8}{15}\gamma_3^{(0)}(R/\Lambda), \tag{78}$$

$$C_2^{(2)} = \frac{64}{63}\gamma_1^{(2)}(R/\Lambda) - \frac{20}{21}\gamma_2^{(2)}(R/\Lambda) + \frac{16}{105}\gamma_3^{(2)}(R/\Lambda), \tag{79}$$

and R/Λ is set to the constant value in (68).

In turbulent channel flow the local Reynolds number can become small in the near-wall region, resulting in increasingly important viscous effects. As a result, Λ in (41) is here modified as

$$\Lambda = \max\left[0.23\frac{k^{3/2}}{\epsilon},\, C_\eta\eta_K\right], \tag{80}$$

where $\eta_K = \left(\nu^3/\epsilon\right)^{1/4}$ is the Kolmogorov length scale and it will be seen that

$$C_\eta = 12.8 \tag{81}$$

gives good agreement with DNS for all Reynolds numbers. Note that in obtaining (80) from (41) we have used $C_\lambda = 0.23$. This value comes from comparison of the exponential $f(r)$ given by (40) with the inertial range form for $f(r)$ obtained from the Kolmogorov hypotheses, as discussed in Ref. [1].

Finally, the eddy viscosity in (77) is written in standard form by

$$\nu_T = C_\mu \frac{k^2}{\epsilon}\,, \tag{82}$$

where here C_μ is given by the realizable Bradshaw hypothesis

$$C_\mu = \begin{cases} 0.09 & \text{for} \quad (Sk/\epsilon) \le 3.4 \\ 0.31(Sk/\epsilon)^{-1} & \text{for} \quad (Sk/\epsilon) > 3.4 \end{cases}\,, \tag{83}$$

and $S \equiv \left[2\overline{S}_{ij}\overline{S}_{ji}\right]^{1/2}$. Since $C_\mu \equiv -\alpha_2/2\alpha_1$ and α_1 depends on P/ϵ as in (48), C_μ must be limited in regions where P/ϵ becomes large. In reality, the evolutions of P/ϵ and Sk/ϵ are closely linked, and the realizable C_μ in (83) provides a relatively straightforward way of accounting for the dependence of C_μ on P/ϵ. Use of (83) is particularly important in turbulent channel flow, since Sk/ϵ becomes large in the near-wall region and reaches a maximum value of $Sk/\epsilon \approx 18$ at $y^+ \approx 8$ as shown in Figure 2.

Figure 3 compares the shear anisotropy a_{12} as a function of y^+ predicted by (77)-(83) with results from DNS. Results from the standard $k-\epsilon$ (SKE) model from (7) and (82) with $C_\mu = 0.09$, and the realizable $k-\epsilon$ (RKE) model from (7) with C_μ given by (83) are also shown. The SKE model shows good agreement with DNS in the centerline of the channel, but dramatically over-predicts the anisotropy magnitude in the near-wall region. The RKE model shows somewhat improved agreement in the near-wall region due to the realizable C_μ in (83), which limits the anisotropy magnitude when Sk/ϵ becomes large near the wall. However, the RKE model fails to capture the decrease in the anisotropy magnitude as the wall is approached. By contrast, the closure in (77)-(83) agrees with the DNS results for all Reynolds numbers down to $y^+ \approx 16$, at which point the present closure begins to over-predict the anisotropy magnitude.

The poor agreement between the present closure and DNS for $y^+ < 16$ could be due to a number of factors, in particular the neglect of inhomogeneities in the turbulence variables, the neglect of the anisotropy in the dissipation tensor ϵ_{ij} (which can become significant as the local Reynolds number decreases in the near-wall region), and the increasingly two-dimensional nature of the turbulence near the wall. While the closure in (77)-(83) does not explicitly address any of these effects, we can obtain a closure that agrees with DNS for $y^+ < 16$ by combining the present approach with prior *ad hoc* wall damping functions. Here we introduce the blending function ϕ, given by

$$\phi = \frac{1}{2} - \frac{1}{2}\tanh\left[a\left(y^+ - b^+\right)\right]\,, \tag{84}$$

and write the eddy viscosity from (82) as

$$\nu_T = f_\mu^{(\phi)} C_\mu \frac{k^2}{\epsilon}\,, \tag{85}$$

where C_μ is still given by (83) and $f_\mu^{(\phi)}$ is a wall damping function given here in van Driest form as

$$f_\mu^{(\phi)} = 1 - \phi \exp\left(-\frac{y^+}{A^+}\right)\,. \tag{86}$$

The anisotropy is then given from the $N = 2$ truncation of (71) by

$$a_{ij} = -2\frac{\nu_T}{k}\left[\overline{S}_{ij} + (1-\phi)\frac{C_2^{(2)}}{\left(C_2^{(1)} - 4/3\right)}\Lambda^2\nabla^2\overline{S}_{ij}\right]\,. \tag{87}$$

The blending function ϕ is 0 for $y^+ > b^+$ and 1 for $y^+ < b^+$, and thus $f_\mu^{(\phi)} = 1$ and $(1-\phi) = 1$ in (87) far from the wall. Near the wall, where the present nonlocal contribution to a_{ij} becomes inaccurate as shown in Fig. 3, the nonlocal Laplacian term in (87) is neglected due to $(1-\phi) = 0$ for $y^+ < b^+$ and the eddy viscosity is damped as in (85) by the underlying wall damping function from (86). For the constants

$$a = 6\,, \quad b^+ = 16\,, \quad A^+ = 26\,, \tag{88}$$

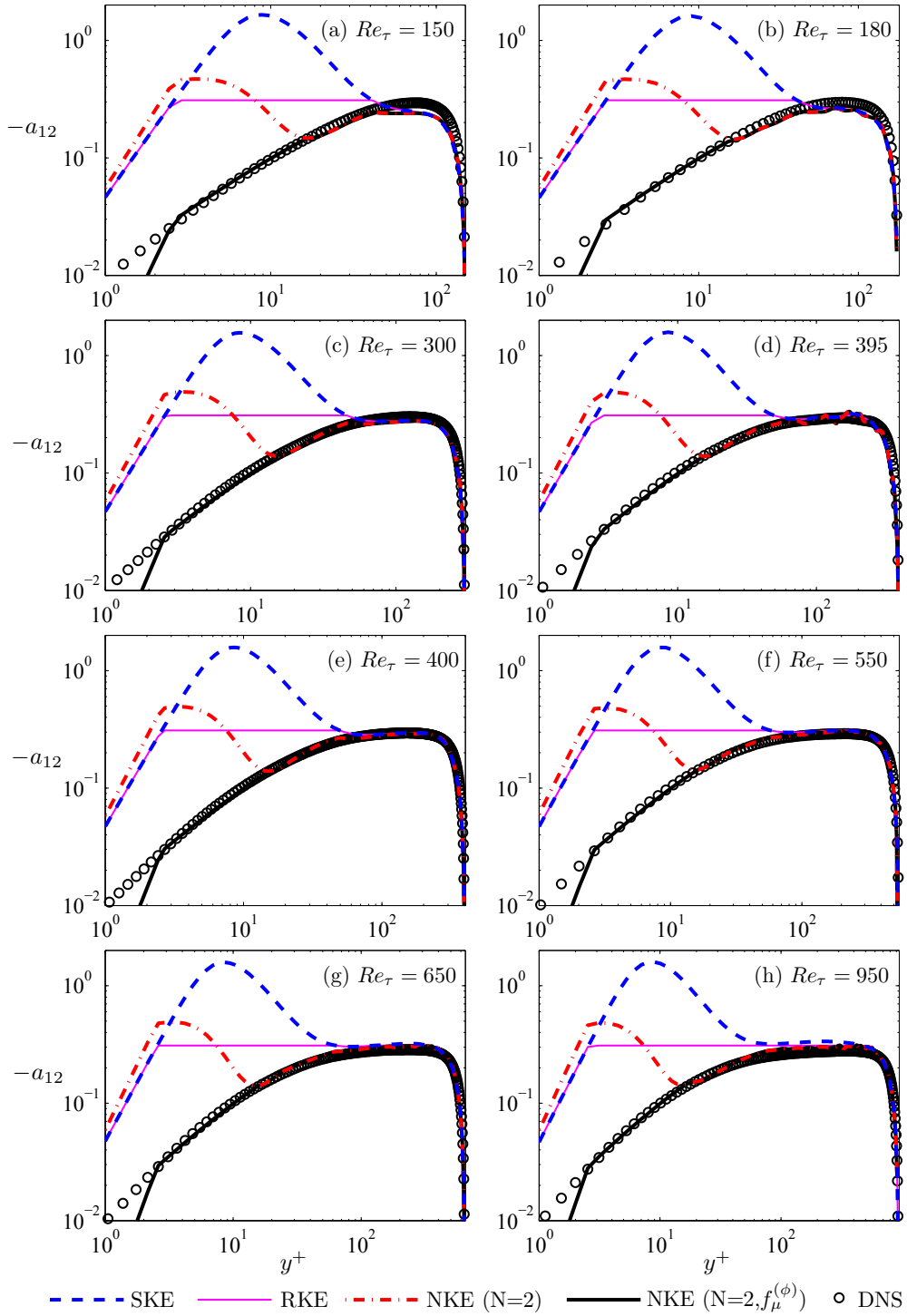

Figure 3. Shear anisotropy $-a_{12}$ as a function of y^+ for $Re_\tau = 150$ (a), $Re_\tau = 180$ (b), $Re_\tau = 300$ (c), $Re_\tau = 395$ (d), $Re_\tau = 400$ (e), $Re_\tau = 550$ (f), $Re_\tau = 650$ (g), and $Re_\tau = 950$ (h) in fully-developed turbulent channel flow. Results from the standard $k-\epsilon$ (SKE) model, the realizable $k-\epsilon$ (RKE) model, the nonlocal $k-\epsilon$ (NKE) model with $N = 2$ given in (77)-(83), and the NKE model with $N = 2$ and $f_\mu^{(\phi)}$ in (84)-(88) are compared with DNS results from Iwamoto *et al.*[19] ($Re_\tau = 150, 300, 400, 650$), Moser *et al.*[20] ($Re_\tau = 180, 395$), and Hoyas and Jimenez[21] ($Re_\tau = 550, 950$). Legend is given at bottom of figure.

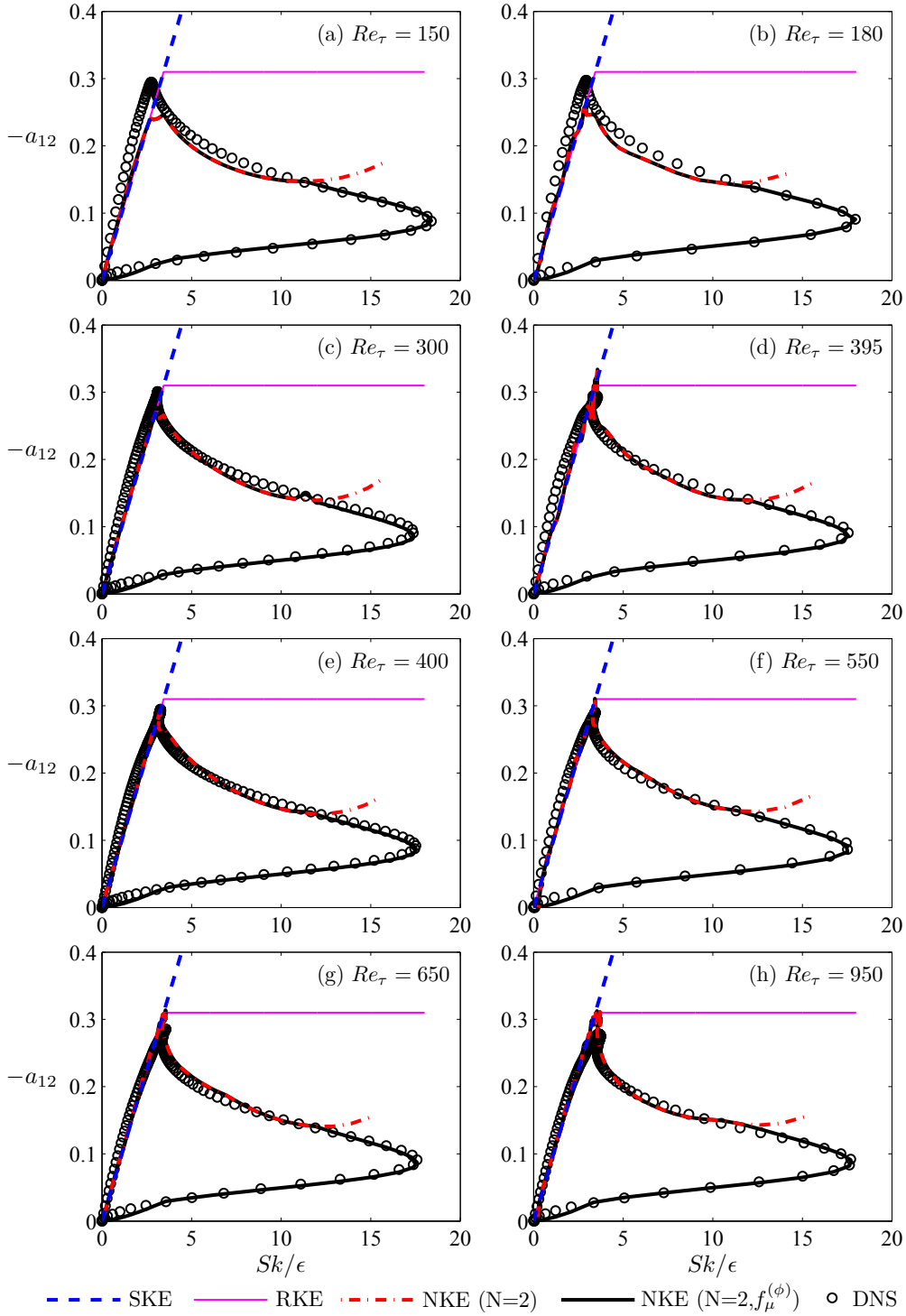

Figure 4. Shear anisotropy $-a_{12}$ as a function of Sk/ϵ for $Re_\tau = 150$ (a), $Re_\tau = 180$ (b), $Re_\tau = 300$ (c), $Re_\tau = 395$ (d), $Re_\tau = 400$ (e), $Re_\tau = 550$ (f), $Re_\tau = 650$ (g), and $Re_\tau = 950$ (h) in fully-developed turbulent channel flow. Results from the standard $k-\epsilon$ (SKE) model, the realizable $k-\epsilon$ (RKE) model, the nonlocal $k-\epsilon$ (NKE) model with $N = 2$ given in (77)-(83), and the NKE model with $N = 2$ and $f_\mu^{(\phi)}$ in (84)-(88) are compared with DNS results from Iwamoto *et al.*[19] ($Re_\tau = 150, 300, 400, 650$), Moser *et al.*[20] ($Re_\tau = 180, 395$), and Hoyas and Jimenez[21] ($Re_\tau = 550, 950$). Legend is given at bottom of figure.

Figure 3 shows that the present nonlocal Laplacian term can be smoothly blended with the wall damping function for all Reynolds numbers, where the choice of constants in (88) allows the nonlocal term in (87) to be applied down to $y^+ \approx 16$, at which point the model reverts to the damping function in (86). It should be noted that for $y^+ < 3$, the present blended model shows poor agreement with the DNS results; this is due to the behavior of the damping function in (86) near the wall. Improved agreement might be obtained through the choice of a different formulation for $f_\mu^{(\phi)}$ (a number of alternative wall damping functions are summarized in Ref. [6]), but such modifications will not be considered herein. The primary purpose of the blended nonlocal-$f_\mu^{(\phi)}$ model in (84)-(88) is to provide a closure that allows integration to viscous walls in existing computational frameworks for solving (1)-(3), and Fig. 3 shows that even with the van Driest function in (86) the present blended approach closely agrees with DNS for nearly the entire channel height.

Finally, Figure 4 compares the shear anisotropy a_{12} as a function of the nondimensional shear parameter Sk/ϵ from the present closure approach and the SKE and RKE models with corresponding results from DNS. The dependence of a_{12} on Sk/ϵ is of particular importance because, as the DNS results in Fig. 4 show, the relation between a_{12} and Sk/ϵ becomes highly non-trivial near the wall, whereas the widely-used SKE model incorrectly predicts $a_{12} \propto Sk/\epsilon$ for all Sk/ϵ. Figure 4 shows that the RKE model limits the anisotropy magnitude for large Sk/ϵ, which results in better agreement with the DNS than the SKE model, but still the correct functional dependence of a_{12} on Sk/ϵ is not captured. By contrast, the present closure in (77)-(83) shows good agreement with the DNS even as Sk/ϵ increases, and substantial departures from the DNS results only occur at $y^+ \approx 16$ where $Sk/\epsilon \approx 12$. Consistent with the results in Fig. 3, improved agreement is obtained using the blended nonlocal-$f_\mu^{(\phi)}$ model in (84)-(88).

V. Conclusions

A new Reynolds stress model including nonlocal and nonequilibrium effects in turbulent flows has been obtained. The present closure is based on a recently proposed nonlocal formulation for the rapid pressure-strain correlation, and is obtained as a quasi-linear solution to the anisotropy transport equation. The model is written in a form analogous to the local equilibrium Boussinesq closure in (7), but expresses the anisotropy in terms of the nonlocal, nonequilibrium effective strain rate $\widetilde{S}_{ij}$ defined in (59) or (60). This relatively simple formulation allows straightforward implementation of the present closure in existing two-equation computational frameworks for solving the RANS equations in (1)-(3).

While $\widetilde{S}_{ij}$ is given in complete time-local form by (60), practical considerations of computational resources and stability will require truncation of the infinite series in (60). These truncations impose restrictions on the integration limits of (37) and (57), and the effective strain rate is written in (67) for finite expansion orders N and M. Comparisons of the closure in (58) and (67) with DNS of fully-developed turbulent channel flow show that even for truncation of $\widetilde{S}_{ij}$ in (67) at $N = 2$, the present closure gives good agreement with DNS results down to $y^+ \approx 16$. This is a substantial improvement compared to predictions from the standard and realizable $k - \epsilon$ models, which begin to show disagreements with DNS for $y^+ \approx 60$.

The accuracy of the present approach can be extended to locations less than $y^+ = 16$ by blending the nonlocal behavior of the model with traditional *ad hoc* wall damping functions, as outlined in (84)-(88). Figures 3 and 4 show that the resulting blended model agrees with DNS essentially to the wall (with only small disagreements for $y^+ < 3$ due to the choice of damping function in (86)), and that the transition to the wall damping function at $y^+ = 16$ is relatively smooth. Despite the use of this damping function near the wall, the present approach has the advantage of representing the anisotropy in a physically rigorous manner for much of the channel, thus increasing the capability of the model to capture additional flow physics in more complex flows. Future work will implement the present closure in full computational frameworks for solving (1)-(3) in practical engineering problems.

Acknowledgments

This work was supported, in part, by the Air Force Research Laboratory (AFRL) through the Michigan-AFRL-Boeing Collaborative Center for Aeronautical Sciences (MAB-CCAS) under Award No. FA8650-06-2-3625.

References

[1]Hamlington, P. E. and Dahm, W. J. A., "Nonlocal form of the rapid pressure-strain correlation in turbulent flows." *Submitted to Phys. Rev. E* (also arXiv: 0906.2755), 2009.

[2]Bradshaw, P., Mansour, N. N., and Piomelli, U., "On local approximations of the pressure-strain term in turbulence models." *Proc. Summer Program, Center for Turbulence Research, Stanford University / NASA Ames Research Center*, 1987, pp. 159–164.

[3]Hamlington, P. E. and Dahm, W. J. A., "Reynolds stress closure for nonequilibrium effects in turbulent flows." *Phys. Fluids*, Vol. 20, 2008, 115101.

[4]Bardina, J., Ferziger, J. H., and Reynolds, W. C., "Improved turbulence models based on large-eddy simulation of homogeneous, incompressible turbulent flows." *Rep. No. TF-19*, Vol. Stanford University, 1983.

[5]Yu, D. and Girimaji, S. S., "Direct numerical simulations of homogeneous turbulence subject to periodic shear." *J. Fluid Mech.*, Vol. 566, 2006, pp. 117–151.

[6]Speziale, C. G. and So, R. M. C., *The Handbook of Fluid Dynamics*, chap. 14, Turbulence Modeling and Simulation, Springer, 1998, pp. 14.1–14.111.

[7]Gatski, T. B. and Jongen, T., "Nonlinear eddy viscosity and algebraic stress models for solving complex turbulent flows." *Prog. Aero. Sci.*, Vol. 36, 2000, pp. 655–682.

[8]Pope, S. B., *Turbulent Flows.*, Cambridge University Press., 2000.

[9]Chou, P. Y., "on velocity correlations and the solutions of the equations of turbulent fluctuation." *Qrtly. of Appl. Math.*, Vol. 3, 1945, pp. 38–54.

[10]Mansour, N., Kim, J., and Moin, P., "Reynolds-stress and dissipation rate budgets in a turbulent channel flow." *J. Fluid Mech.*, Vol. 194, 1988, pp. 15–44.

[11]Launder, B. E., Reece, G., and Rodi, W., "Progress in the development of a Reynolds stress turbulence closure." *J. Fluid Mech.*, Vol. 68, 1975, pp. 537–566.

[12]Speziale, C. G., Sarkar, S., and Gatski, T. B., "Modeling the pressure strain correlation of turbulence: an invariant dynamical systems approach." *J. Fluid Mech.*, Vol. 227, 1991, pp. 245–272.

[13]Gatski, T. B. and Speziale, C. G., "On explicit algebraic stress models for complex turbulent flows." *J. Fluid Mech.*, Vol. 254, 1993, pp. 59–78.

[14]Girimaji, S. S., "Fully explicit and self-consistent algebraic Reynolds stress model." *Theoret. Comput. Fluid Dyn.*, Vol. 8, 1996, pp. 387–402.

[15]Wallin, S. and Johansson, A. V., "An explicit algebraic Reynolds stress model for incompressible and compressible turbulent flows." *J. Fluid Mech.*, Vol. 403, 2000, pp. 89–132.

[16]Rotta, J., "Statistische theorie nichthomogener turbulenz," *Z. fur Phys.*, Vol. 129, 1951, pp. 547–572.

[17]Hamlington, P. E. and Dahm, W. J. A., "Frequency response of periodically sheared homogeneous turbulence." *Phys. Fluids*, Vol. 21, 2009, 055107.

[18]Hamlington, P. E., Schumacher, J., and Dahm, W. J. A., "Direct Assessment of Vorticity Alignment with Local and Nonlocal Strain Rates in Turbulent Flows," *Phys. Fluids*, Vol. 20, 2008, 111703.

[19]Iwamoto, K., Suzuki, Y., and Kasagi, N., "Reynolds number effect on wall turbulence: Toward Effective Feedback Control," *Int. J. Heat and Fluid Flow*, Vol. 23, 2002, pp. 678–689.

[20]Moser, R. D., Kim, J., and Mansour, N. N., "Direct numerical simulation of turbulent channel flow up to $Re_\tau = 590$." *Phys. Fluids*, Vol. 11, 1999, pp. 943.

[21]Hoyas, S. and Jimenez, J., "Reynolds number effects on the Reynolds-stress budgets in turbulent channels." *Phys. Fluids*, Vol. 20, 2008, 101511.